Research Article

Journal of Environmental Nanotechnology

Nanoparticle-reinforced Aluminium Matrix Hybrid Composites: Processing and Characterization

Shriyash S. Shinde* and Shivprakash B. Barve

Department of Mechanical Engineering, Dr. Vishwanath Karad MIT World Peace University, Kothrud, Pune, MH, India

Received: 10.01.2026 Accepted: 05.02.2026 Published: 30.03.2026

*shinde17.shri@gmail.com

ABSTRACT

In the pursuit of high-performance materials for demanding applications, the development of hybrid composites has emerged as a breakthrough solution. In the present work, A356 matrix hybrid nanocomposites reinforced with boron carbide (B_4C) (1, 2, 3, 4, and 5 wt.%) and zirconium dioxide (ZrO_2) (1 wt.% constant) were produced by the two-step stir casting technique assisted by ultrasonic vibrations. Microstructure, mechanical characteristics, and tribological behaviour of A356–B_4C–ZrO_2 hybrid composites were investigated. The impact of T6 heat treatment on the mechanical characteristics of the prepared composites was also examined. The microhardness, yield strength, and ultimate tensile strength of the hybrid composites showed improvements of 35%, 66%, and 60%, respectively, compared to the A356 matrix. The fracture morphology of the hybrid nanocomposites was analyzed using scanning electron microscopy. The even dispersion of nanoparticles achieved through mechanical stirring and ultrasonic vibration assistance, along with microstructural changes such as precipitation hardening and spheroidization of silicon particles due to thermal treatment, significantly lowered the wear rate and friction coefficient.

Keywords: A356; Hybrid nanocomposites; Stir casting; Characterization; Wear.

1. INTRODUCTION

The increasing demand for sustainable engineering solutions has intensified research into lightweight, high-performance materials (Chak *et al.* 2020). Aluminium's notable benefit lies in its exceptional simplicity of being fabricated into any desired shape. Aluminium and its alloys are low-cost, versatile materials with properties suitable for applications in aerospace, automotive, construction, cookware, electronics, cryogenics, and more (Kammer, 2018). A356 has been extensively employed in aerospace, automobiles, structural, military, and other applications where high-strength permanent mould or castings are needed (Chandla *et al.* 2020). Improving mechanical properties and wear resistance is crucial to broaden the use of these castings in demanding conditions. Several methods, such as gravity die casting, centrifugal casting, melt infiltration, compo casting, liquid-state stir casting, powder metallurgy and sintering, laser deposition, and solid-state deformation processing, have been developed to prepare aluminium matrix composites (AMCs) (Fanani *et al.* 2021). Stir casting remains one of the most practical methods for fabricating AMCs owing to its reliability, affordability, ease of use, and suitability for large-scale production (Borisade *et al.* 2023). In the last three decades, considerable work has been undertaken to improve the performance and characteristics of AMCs by including reinforcements like Al_2O_3 (Awate and Barve, 2022a), TiO_2 (Kumar *et al.* 2023), SiO_2 (Azadi *et al.* 2020), ZnO (Moona *et al.* 2018), Si_3N_4 (Fayomi *et al.* 2020), SiC (Akbar *et al.* 2020), TiC (Balamurugan *et al.* 2023; Sambathkumar *et al.* 2023), B_4C (Kumar *et al.* 2021), CNT (Casati and Vedani, 2014), graphene (Tabandeh *et al.* 2016; Boppana *et al.* 2020) TiB_2 (Sambathkumar *et al.* 2023), ZrB_2 (Kumar and Kumar, 2024), red mud (Bhoi *et al.* 2020), ZrO_2 (Oyewo *et al.* 2024) and fly ash (Sahu and Sahu, 2020), using stir casting technique. By combining two or more types of reinforcement particles, hybrid composites achieve a unique set of properties that can meet design requirements more efficiently and affordably than traditional composites (Manda *et al.* 2022). The benefits of hybrid composites over traditional ones include improved mechanical and thermal characteristics, and reduced density and cost (Singh *et al.* 2022).

(Sharma *et al.* 2019a) investigated the effects of T4 and T6 heat treatments on LM30 with sillimanite inclusions fabricated by stir casting. The T6 heat-treated composite exhibited enhanced hardness compared to other composites. The lower value of the coefficient of friction was reported for T6 heat-treated composites. (Kumar and Kumar, 2024) have investigated hybrid AMCs with ZrB_2 and fly ash reinforcements and an AA7075 matrix, followed by T6 heat treatment. The mechanical characterization has shown improved results. The tensile strength and hardness of hybrid composites have shown 109% and 77%, compared to the matrix alloy. (Balamurugan *et al.* 2023) have developed an Al6061 matrix hybrid AMC reinforced with TiC and

RHA. TiC wt.% was varied from 3 wt.% to 12 wt.%, while RHA concentration was fixed to 3 wt.%. Hybrid composites exhibited improved tensile strength, hardness, and flexural strength. The inclusion of TiC particles enhanced the erosion resistance of the hybrid composite. B_4C is an exceptional reinforcement material for AMCs owing to its remarkable characteristics, including extremely high hardness and stiffness. Additionally, it offers superior wear resistance and excellent chemical stability, making it a top choice compared to other ceramics (Chandel *et al.* 2021; Kumar *et al.* 2021; Çanakçı *et al.* 2024; Chandrashekar *et al.* 2024). ZrO_2 provides high-temperature strength, enhances mechanical and wear performance, improves crack resistance, and serves as an effective spacer to prevent particle agglomeration (Khalili *et al.* 2020; Pandiyarajan *et al.* 2022). Adding even a small amount of nanoparticles to AMCs can significantly enhance their functional properties. This allows the composite to achieve high performance with minimal reinforcement (Bhoi *et al.* 2020). Nano-sized reinforcements enhance interfacial interactions, strength, fatigue life, machinability, and high-temperature creep resistance without compromising ductility (Shinde and Barve, 2025). Improvements in MMCs arise from hardening, fine particle size, uniform dispersion, optimal inter-particle spacing, and thermal stability (Alam *et al.* 2017). Nano-sized particles can simultaneously enhance the strength and ductility of AMCs relative to the incorporation of micro-sized particles (Geng *et al.* 2018). The even mixing of the nanoparticles in the metal matrix is quite tricky. This is particularly relevant when employing liquid-based processing techniques (Fadavi *et al.* 2015). This can be tackled by effective stirring in two steps with vortex formation using a low-cost stir-casting setup (Ravindra *et al.* 2023).

This study aims to produce aluminium matrix nanocomposites that strike a balance between high strength, wear resistance, and cost-effectiveness in demanding engineering applications. In the present work, A356 matrix nanocomposite with B_4C and ZrO_2 nano-reinforcements was developed using the two-step stir casting. Ultrasonic vibrations of 20 kHz were applied to the mould during the solidification of composites to ensure even distribution of reinforcement particles. The microstructural, mechanical, and tribological characteristics of the T6 heat-treated hybrid composite were examined and discussed.

2. EXPERIMENTATION

2.1 Materials

In the present study, A356 alloy obtained from Parshwamani Metal, Mumbai, India, was employed as the matrix material, comprising 7.50 wt.% Si, 0.35 wt.% Mg, 0.20 wt.% Fe, 0.20 wt.% Cu, and 0.10 wt.% Mn, with the remainder Al. B_4C and ZrO_2 nanopowders (purity 99.5%, particle size 90 nm) were procured from Intelligent Materials Pvt. Ltd., Punjab, India. The B_4C content was varied from 1 to 5 wt.% in 1 wt.% increments, whereas ZrO_2 content was fixed at 1 wt.%.

2.2 Fabrication Process and Heat Treatment

After cleaning and weighing, the aluminium alloy was added to the graphite crucible, and the melting was started. The reinforcement powder was measured, heated, and maintained at a temperature of 500 °C for 50 minutes. At a semisolid state, at 590 °C, hexachloroethane powder was added. This removes entrapped gases from the melt. The scum layer of impurities was removed. 1% magnesium by weight was used to strengthen the bond between the matrix alloy and nano-sized particles. Molten A356 alloy was stirred at 700 °C using a mechanical stirrer (300 rpm, 20 min), during which reinforcements were gradually added as shown in Figure 1. The melt was cooled to a semi-solid state, reheated to 800 °C, and then subjected to a second stirring for 12 min. It was then poured into a mould placed on a non-contact ultrasonic vibrator (20 kHz) during solidification. This procedure was repeated for all hybrid composite concentrations.

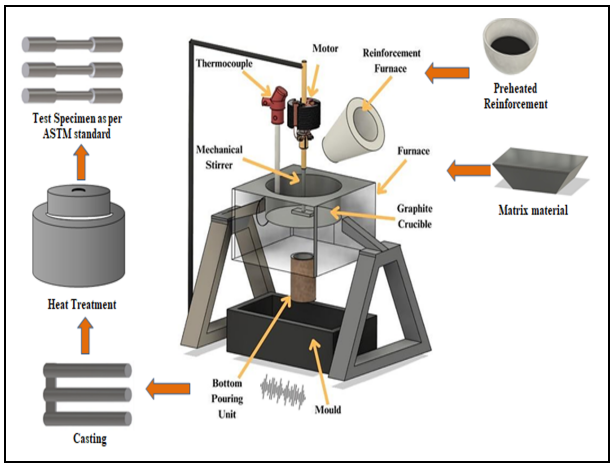


Fig. 1: Experimental procedure for the production of heat-treated A356-B_4C-ZrO_2 hybrid composites

Following casting, all samples underwent a T6 heat treatment. The cast samples were put in an electric furnace with temperature control for the heat treatment process. The solution heat treatment was performed at 485 °C for 2 h, followed by quenching in room-temperature water. The samples were then artificially aged at 160 °C for 6 h before air cooling. After heat treatment, the samples were cut and mechanically polished according to ASTM standards.

3. CHARACTERIZATION

For microstructural characterization, specimens were prepared by grinding, polishing, and etching cast samples. An optical microscope (Olympus DX1000) was utilized to examine the microstructure of the prepared hybrid composite. The morphology of the developed specimens was examined using scanning electron microscopy (SEM, FEI Nova 450) coupled with energy-dispersive spectroscopy (EDS, Bruker XFlash 6I30). The phase composition of the prepared hybrid composites was analyzed using X-ray diffraction (XRD, D8 Advance Diffractometer) with Cu Kα radiation (λ = 1.541874 Å). The microhardness of the prepared specimens was measured using a Vickers microhardness tester (FSA, FMV1-AC-AT) in accordance with ASTM E384. Tensile testing was conducted using an FSA M100 computer-controlled universal testing machine at a constant crosshead speed of 1 mm/min. Each test was performed three times to ensure consistent and reliable results. The wear characteristics were assessed using a pin-on-disc tester (DUCOM TR-20LE) in accordance with ASTM G99. An EN31 steel disc (diameter 110 mm) was used against composite pins (diameter 8 mm and length 30 mm), as shown in Figure 2. Tests were performed at 50 N load, 3.0 m/s sliding speed, and 120 mm track diameter under ambient conditions. The wear rate was obtained from the average of three trials, calculated from the change in specimen height relative to the original cross-sectional area. Additionally, the worn surfaces were examined using SEM.

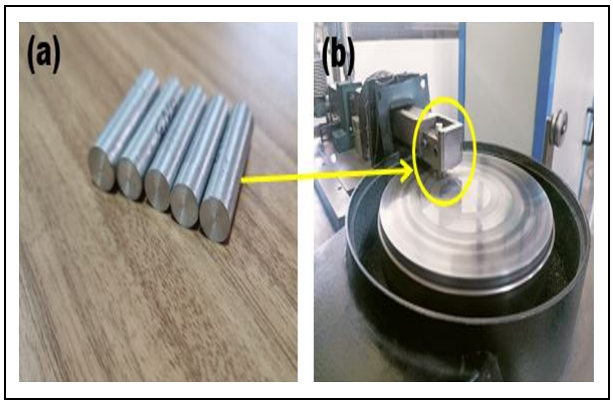


Fig. 2: Wear testing of pure A356 alloy and hybrid composites: (a) prepared test specimens, and (b) specimen placement on the test rig

4. RESULTS AND DISCUSSION

4.1 Optical Microscopy and EDS Analysis

Figure 3 shows the optical microstructure of the T6 heat-treated pure A356 alloy and hybrid composites. The images reveal a uniform dispersion of reinforced phases within the aluminium matrix. The B_4C particles appear as dark, angular features, while ZrO_2 particulates exhibit a more rounded morphology. Eutectic silicon appears in a moderately modified flake form, evenly distributed throughout the matrix. The colour contrast in the etched micrograph highlights the multiphase interactions and grain structure, indicating adequate wetting and minimal clustering. The observed microstructure indicates an even particle distribution of reinforcement particles, strong interfacial bonding, and negligible agglomeration. This outcome stems from the combined influence of two-step stirring and ultrasonic vibrations, which enhanced melt homogenization through cavitation and acoustic streaming during solidification.

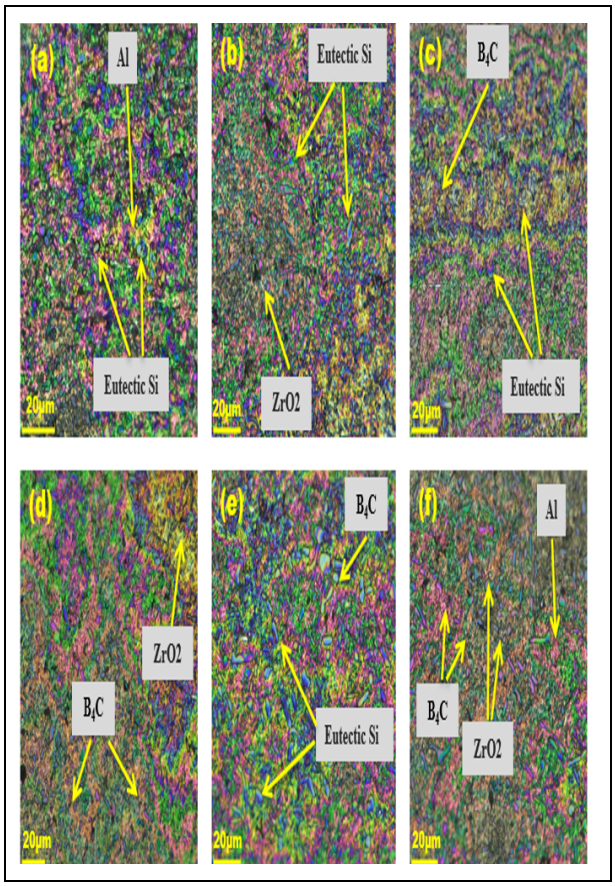


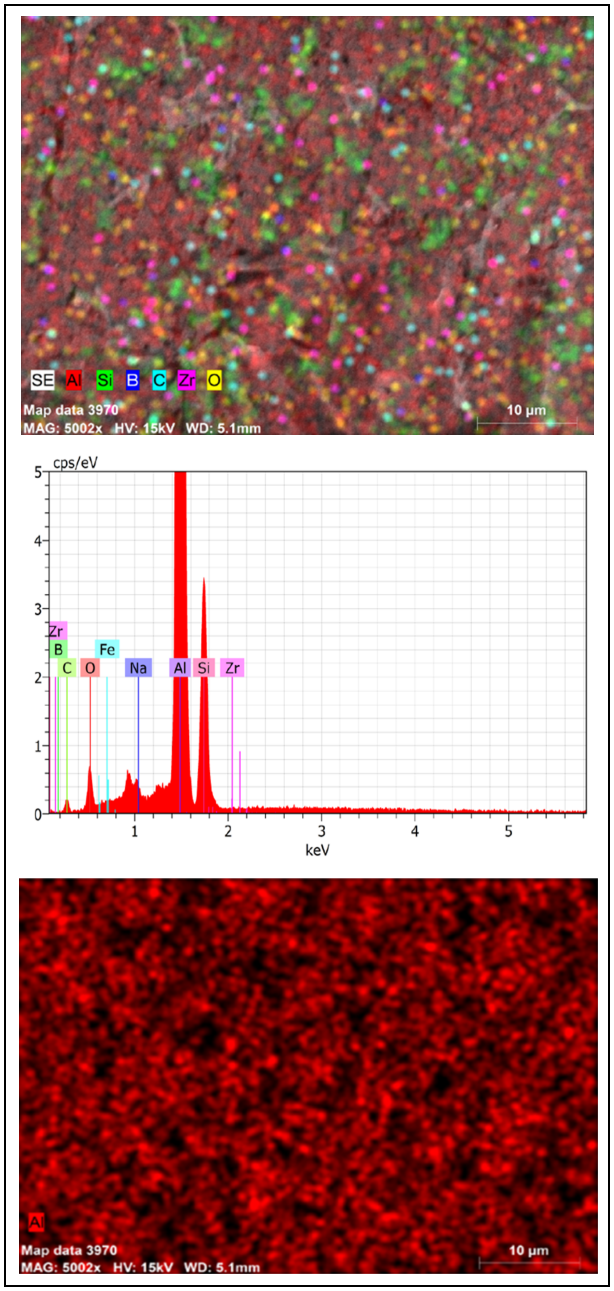
Fig. 3: Optical morphologies of: (a) Pure A356 alloy and hybrid composites, (b) 1% B_4C and 1% ZrO_2, (c) 2% B_4C and 1% ZrO_2, (d) 3% B_4C and 1% ZrO_2, (e) 4% B_4C and 1% ZrO_2, and (f) 5% B4C and 1% ZrO_2

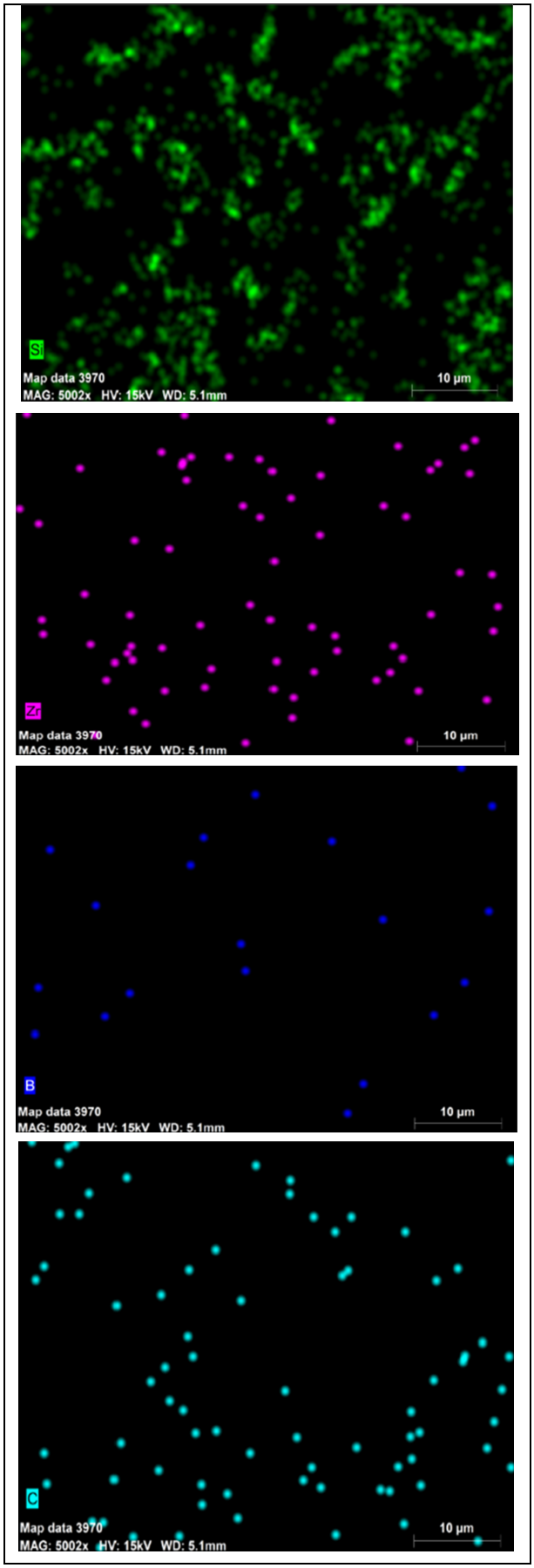
Figure 4 confirms the existence of Al, Si, B, C, Zr, and O elements across the A356 matrix. This proves the uniformity and consistency of B_4C and ZrO_2 nanoparticles within the A356 matrix hybrid composite fabricated via the two-step stir casting method.

4.2 XRD Analysis

The X-ray diffraction examination (Figure 5) of the prepared composites reveals the presence of multiple

crystalline phases. The dominant peaks correspond to the aluminium matrix, with characteristic reflections at 2θ = 38°, 65°, and 78°. With increasing B_4C content (1–5 wt.%), clear secondary peaks appear near 44°, indicating the successful incorporation of boron carbide as a reinforcement phase. Additionally, consistent peaks observed near 28° across all samples indicate the presence of ZrO_2, which was added at a constant 1 wt.%. A minor contribution from silicon is also possible around 28°, overlapping with ZrO_2. The increasing intensity of B_4C peaks reflects successful integration and dispersion of the reinforcement particles, without compromising the matrix crystallinity. The absence of any amorphous humps further confirms the good crystallinity and phase stability of the developed composite system.





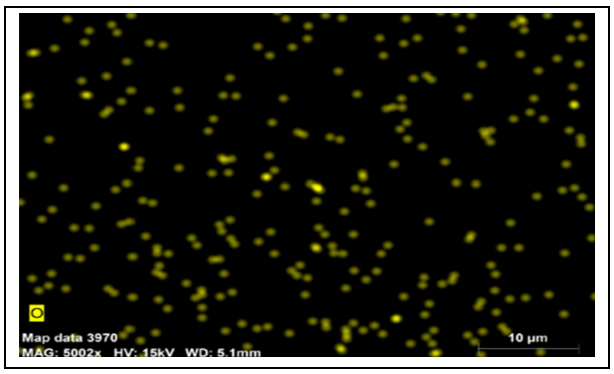


Fig. 4: Mapping data of EDS test of hybrid composite with 3% B4C and 1% ZrO_2: (a) Distribution of the elements Al, Si, B, C, Zr, and O, (b) Peaks of the elements Al, Si, B, C, Zr, and O, (c) Dispersion of Al, (d) Dispersion of Si, (e) Dispersion of Zr, (f) Dispersion of B, (g) Dispersion of C, and (h) Dispersion of O across the matrix

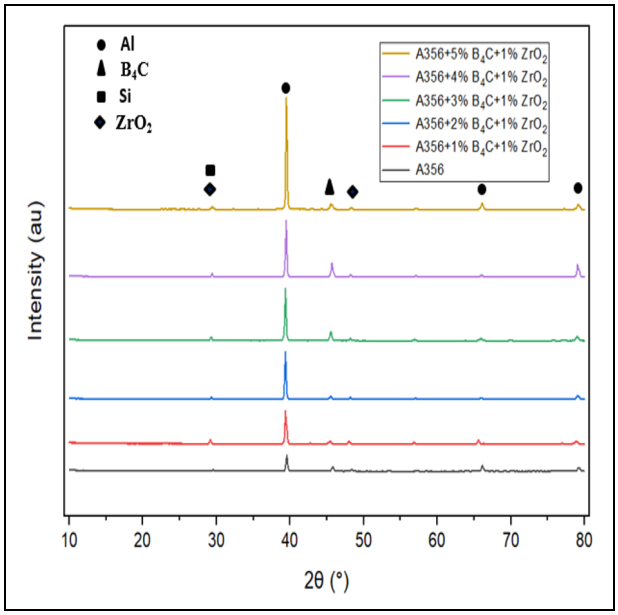


Fig. 5: XRD patterns of heat-treated pure A356 alloy and A356-B_4C-ZrO_2 hybrid composites

4.3 Microhardness Testing

Figure 6 illustrates the relationship between microhardness and nano-B_4C and nano-ZrO_2 concentrations in the A356 matrix. The micro-Vickers hardness test revealed improvement in the hardness of the hybrid composites compared to the pure A356 alloy. The microhardness of the hybrid composite is 161 HV, indicating a 35% increase compared to the microhardness of the pure A356 alloy, which is 119 HV. The hardness improved with the addition of nano-B_4C particles, attributed to their high hardness and uniform dispersion in the matrix. T6 heat treatment further enhanced hardness, which strengthened the aluminium matrix. Dispersion strengthening plays a dominant role, where nano-sized B_4C particles impede dislocation motion through the Orowan mechanism, increasing critical stress for deformation (Kumar *et al.* 2021). The T6 treatment further amplified hardness by precipitating fine Mg_2Si phases, which acted as additional barriers to dislocations (Awate and Barve, 2022b). The alloy was strengthened as a result of these precipitates. The heat treatment process diminished the elongated structures, resulting in the creation of more rounded, spheroidal forms. Quenching secured these structures, whereas artificial ageing enhanced the silicon morphology.

Additionally, grain refinement during stir casting promoted Hall-Petch strengthening. The thermal mismatch between reinforcements and the aluminium matrix generated dislocations at the particle-matrix interface, contributing to strain hardening (Sharma *et al.* 2019b). Ultrasonic-assisted stir casting ensured uniform nanoparticle dispersion, improving load transfer to the rigid reinforcements. Consistent hardness across the composites confirmed uniform distribution and process control. Tensile testing was performed on hybrid nanocomposites with varying proportions of B_4C and ZrO_2 reinforcements. Figure 7 depicts the tensile strength response of pure A356 alloy and hybrid composite samples.

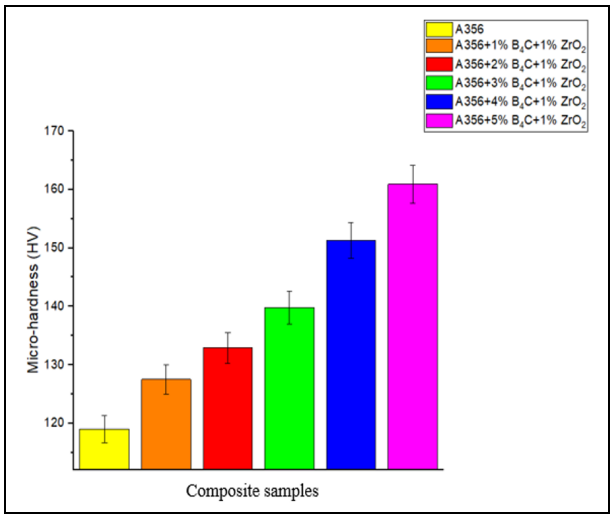


Fig. 6: Microhardness of T6 heat-treated pure A356 alloy and A356–B_4C–ZrO_2 hybrid composites

4.4 Tensile Strength

The improvement in yield strength YS and UTS of composites results from: (i) the reinforcement percentage, (ii) the interface bonding between the matrix and the reinforcement, and (iii) reinforcement dispersion within the matrix (Pingale *et al.* 2020). The present study's improvement in YS and UTS can be ascribed to the even spread of hybrid reinforcements, adequate bonding at the interface between the reinforcements and A356 matrix, and heat treatment, leading to adequate

interfacial load transfer capabilities. Heat treatment caused silicon particles to fragment and spheroidize, enhancing the tensile properties of the specimens.

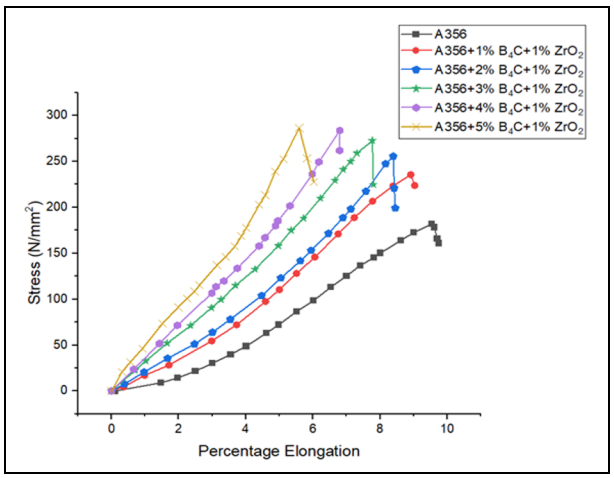


Fig. 7: Stress vs. percentage elongation curves of heat-treated pure A356 alloy and hybrid composites

Table 1. Tensile strengths of heat-treated pure A356 alloy and hybrid composites

Samples	YS (MPa)	UTS (MPa)
A356 alloy	142	179
A356+1%B_4C+1%ZrO_2	190	235
A356+2%B_4C+1%ZrO_2	198	256
A356+3%B_4C+1%ZrO_2	214	272
A356+4%B_4C+1%ZrO_2	229	282
A356+5%B_4C+1%ZrO_2	236	286

4.5 Fractography

Figure 8 shows fractured surfaces of the prepared hybrid composites. Figure 8b shows several voids containing entrapped nanoparticles. Cup-like dimples indicate ductile deformation, while particle cracking, pullouts, and micro-cracks suggest localized plastic deformation. The presence of reinforcement particles in voids (Figures 8b–d) demonstrates strong interfacial bonding between the matrix and reinforcements. T6 heat treatment improved tensile properties by enhancing load transfer from the matrix to the reinforcement particles, which strengthens the composite. The matrix also contains voids and micro-cracks (Figure 8c) that act as fracture initiation sites. Fractography of the tensile specimens revealed a mixed-mode fracture, combining ductile and plastic features, with rupture as the failure mode.

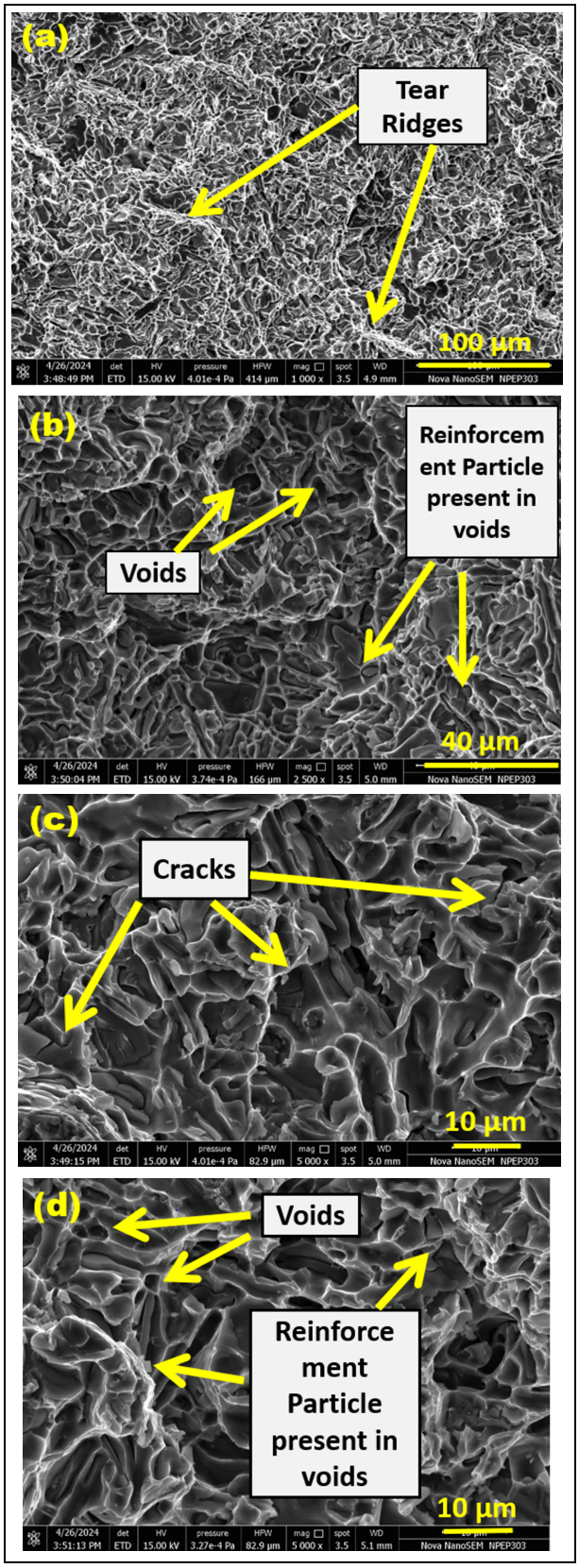


Fig. 8: FESEM images of fracture surfaces: (a) pure A356 alloy and hybrid composites, (b) 2% B_4C and 1% ZrO_2, (c) 3% B_4C and 1% ZrO_2, and (d) 4% B_4C and 1% ZrO_2

4.6 Wear Behavior

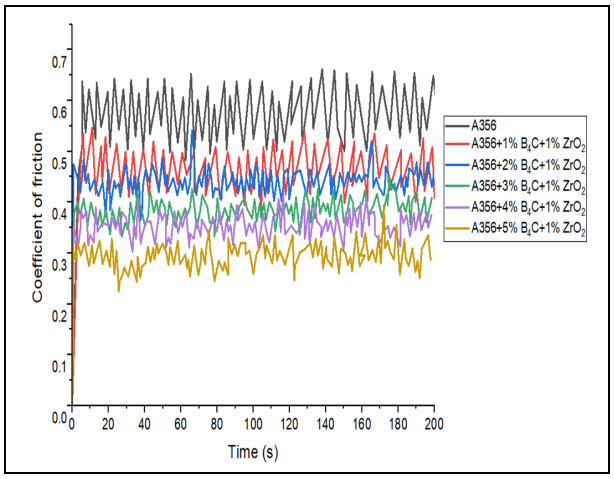


Fig. 9 (a): Friction coefficient variation of the unreinforced A356 matrix and hybrid nanocomposites

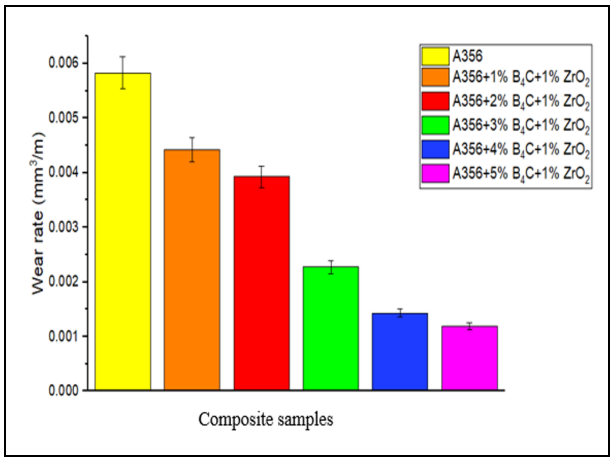
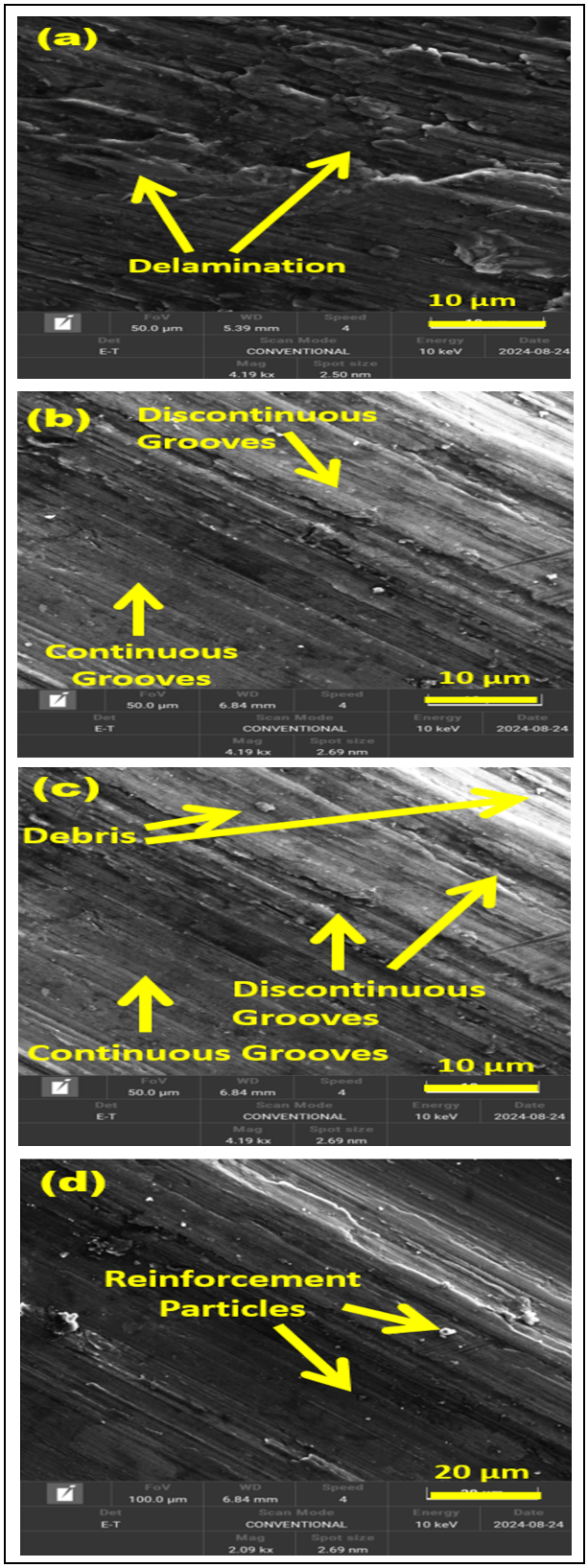


Fig. 9 (b): Wear rates of heat-treated pure A356 alloy and hybrid composites

Figure 9 (a) shows the variation of the friction coefficient for the base alloy and the hybrid nanocomposites. All the friction coefficient curves advance quickly before stabilizing. The friction coefficient decreased from 0.58 to 0.31 as the B_4C content in the matrix increased from 0 to 5%, with the ZrO_2 percentage kept constant. The wear behavior of pure A356 alloy and hybrid composites is examined (Figure 9b), keeping the load, sliding distance, and speed constant. The lack of hard ceramic particles in the matrix leads to a higher wear rate in the base alloy. The wear rate of hybrid composites decreased with an increase in the weight percentage of nano-reinforcements. The hybrid composite demonstrated a 76% reduction in wear rate and a 49% lower coefficient of friction compared to the unreinforced base alloy, highlighting its superior tribological performance. SEM images of the worn surfaces revealed continuous and discontinuous grooves, characteristic of abrasive wear, in Figure 10. Delamination dominated the wear process with an applied load of 50 N. The enhancement in wear resistance can be ascribed to the even dispersion of nano-reinforcing particles assisted by ultrasonic vibration, as well as precipitation hardening and the spheroidization of silicon particles resulting from the T6 heat treatment.



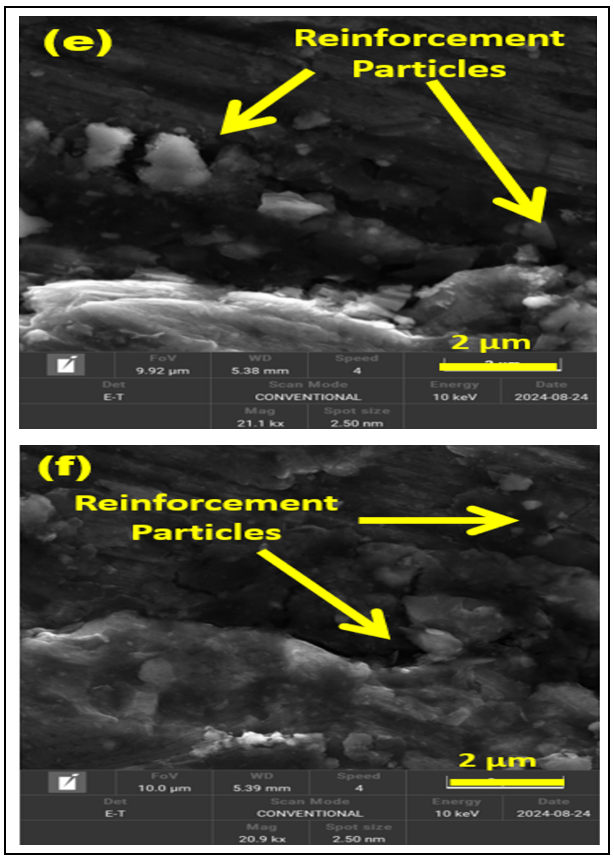


Fig. 10: SEM micrographs of the worn surface during the wear testing: (a) pure A356 alloy and hybrid composites, (b) 1% B_4C and 1% ZrO_2, (c) 2% B_4C and 1% ZrO_2, (d) 3% B_4C and 1% ZrO_2, (e) 4% B_4C and 1% ZrO_2, and (f) 5% B_4C and 1% ZrO_2

5. CONCLUSION

The A356 matrix hybrid nanocomposite was successfully manufactured by ultrasonic vibration-assisted two-step stir casting with negligible clustering. The microstructural examination, including FESEM, EDS, and XRD analyses, confirms the incorporation of B_4C and ZrO_2 nanoparticles in the base matrix. The reinforcements are uniformly distributed and well-bonded, owing to the combined effect of controlled stirring and ultrasonic vibration assistance during the casting process. The micro-Vickers hardness, YS, and UTS of the A356–B_4C–ZrO_2 hybrid composites improved with the addition of nano-B_4C and nano-ZrO_2. With the concentration of nano-B_4C 5 wt.% and ZrO_2 1 wt.% in the A356 matrix, the microhardness of 161 HV, YS of 265 MPa, and UTS of 286 MPa were recorded, revealing increases of 35%, 66%, and 60%, respectively. The developed hybrid nanocomposites exhibited a superior tensile strength while maintaining comparable hardness values, indicating the retention of ductility. Fractographic analysis of the tensile-tested specimens revealed a mixed fracture mode characterized by features of both ductile failure and plastic deformation. In tribological performance, the developed hybrid composite showed significant wear resistance, with wear rate and friction coefficient reduced by 76% and 49%, respectively, relative to the base alloy. The T6 heat treatment modified the morphology of eutectic silicon, transforming it into a more spheroidized form. The quenching step preserved this refined structure, while subsequent artificial ageing further improved the silicon morphology and its distribution within the matrix. The A356–B_4C–ZrO_2 hybrid composites synthesized using the proposed approach are expected to be suitable for cast components in the automotive, aerospace, sports equipment, and industrial sectors owing to their superior mechanical and tribological characteristics.

ACKNOWLEDGEMENT

The authors gratefully acknowledge Pimpri Chinchwad College of Engineering, Pune, India, for providing the mechanical testing facility and Savitribai Phule Pune University (SPPU), India, for access to the XRD, SEM, and EDS facilities. The authors also wish to acknowledge the Department of Mechanical Engineering, Dr. Vishwanath Karad, MIT-WPU, Pune, India, for providing the wear testing facility that supported this work.

FUNDING

This research received no specific grant from any funding agency in the public, commercial, or not-for-profit sectors.

CONFLICTS OF INTEREST

The authors declare that there is no conflict of interest.

COPYRIGHT

This article is an open-access article distributed under the terms and conditions of the Creative Commons Attribution (CC BY) license (http://creativecommons.org/licenses/by/4.0/).

REFERENCES

Akbar, H. I., Surojo, E., Ariawan, D., Putra, G. A. and Wibowo, R. T., Effect of reinforcement material on properties of manufactured aluminum matrix composite using stir casting route, *Procedia Struct. Integr.*, 27(2019), 62–68(2020). https://doi.org/10.1016/j.prostr.2020.07.009

Alam, M. T., Ansari, A. H., Arif, S. and Alam, M. N., Mechanical properties and morphology of aluminium metal matrix nanocomposites-stir cast products, *Adv. Mater. Process Technol.*, 3(4), 600–615(2017). https://doi.org/10.1080/2374068X.2017.1350543

Awate, P. P. and Barve, S. B., Microstructural observation and mechanical properties behavior of Al2O3/Al6061 nanocomposite fabricated by stir casting process, *Eng. Res. Exp.*, 4(1), 015023(2022a). https://doi.org/10.1088/2631-8695/ac54ed

Awate, P. P. and Barve, S. B., Enhanced microstructure and mechanical properties of Al6061 alloy via graphene nanoplates reinforcement fabricated by stir casting, *Funct. Compos. Struct.*, 4(1), 015005(2022b). https://doi.org/10.1088/2631-6331/ac586d

Azadi, M., Rezanezhad, S., Zolfaghari, M. and Azadi, M., Investigation of tribological and compressive behaviors of Al/SiO_2 nanocomposites after T6 heat treatment, *Sadhana - Acad. Proc. Eng. Sci.*, 45(1), 28(2020). https://doi.org/10.1007/s12046-019-1257-z

Balamurugan, K., Shanmugam, V., Palani, G., Sundarakannan, R., Sathish, T., Linul, E., Khan, S. A. and Asif, M., Effect of TiC/RHA on solid particle erosion of Al6061 hybrid composites fabricated through a 2-step ultrasonic-assisted stir casting process, *J. Mater. Res. Technol.*, 25, 4888–4900(2023a). https://doi.org/10.1016/j.jmrt.2023.06.225

Bhoi, N. K., Singh, H. and Pratap, S., Developments in the aluminum metal matrix composites reinforced by micro/nano particles – A review, *J Compos Mater*, 54(6), 813–833(2020). https://doi.org/10.1177/0021998319865307

Boppana, S. B., Dayanand, S., Anil Kumar, M. R., Kumar, V. and Aravinda, T., Synthesis and characterization of nano graphene and ZrO_2 reinforced Al 6061 metal matrix composites, *J. Mater. Res. Technol.*, 9(4), 7354–7362(2020). https://doi.org/10.1016/j.jmrt.2020.05.013

Borisade, S. G., Owoeye, S. S., Akindutire, S. and Epstein, H., Effects of alumina-rich waste (valoxy) as an alternative sustainable material to alumina on the morphology, mechanical and wear behavior of Al-6063 alloy by stir casting, *J. Alloys Metall. Syst.*, 3(, 100021(2023). https://doi.org/10.1016/j.jalmes.2023.100021

Çanakçı, A., Karabacak, A. H., Çelebi, M., Özkaya, S. and Arpacı, K. A., A Study on the Optimization of Nano-B4C Content for the Best Wear and Corrosion Properties of the Al-Based Hybrid Nanocomposites,. *Arab. J. Sci. Eng.*, 49(11), 14625-14641(2024). https://doi.org/10.1007/s13369-024-08736-w

Casati, R. and Vedani, M., Metal matrix composites reinforced by Nano-Particles—A review, *Metals*, 4(1), 65–83(2014). https://doi.org/10.3390/met4010065

Chak, V., Chattopadhyay, H. and Dora, T. L., A review on fabrication methods, reinforcements and mechanical properties of aluminum matrix composites, *J. Manuf. Process*, 56, 1059–1074(2020). https://doi.org/10.1016/j.jmapro.2020.05.042

Chandel, R., Sharma, N. and Bansal, S. A., A review on recent developments of aluminum-based hybrid composites for automotive applications, *Emergent Mater.*, 4(5), 1243–1257(2021). https://doi.org/10.1007/s42247-021-00186-6

Chandla, N. K., Yashpal., Kant, S., Goud, M. M. and Jawalkar, C. S., Experimental analysis and mechanical characterization of Al 6061/alumina/bagasse ash hybrid reinforced metal matrix composite using vacuum-assisted stir casting method, *J. Compos. Mater.*, 54(27), 4283–4297(2020). https://doi.org/10.1177/0021998320929417

Chandrashekar, J. R., Chandrashekar, R., Haseebuddin, M. R. and Savitha, Y. L., Effect of Heat Treatment (T6) on Mechanical Behaviour of Double Sized B4C Ceramic Particle Reinforced A356 Composite, *J. Inst. Eng. India. Ser. D.* (2024). https://doi.org/10.1007/s40033-024-00825-2

Fadavi, B. A., Tahamtan, S., Jiang, Z. Y., Wei, D., Yazdani, S., Azari Khosroshahi, R., Taherzadeh, M. R., Xu, J., Zhang, X. and Gong, D., Enhanced tensile properties of aluminium matrix composites reinforced with graphene encapsulated SiC nanoparticles, *Compos. Part Appl. Sci. Manuf.*, 68, 155–163(2015). https://doi.org/10.1016/j.compositesa.2014.10.010

Fanani, E. W. A., Surojo, E., Prabowo, A. R. and Akbar, H. I., Recent progress in hybrid aluminum composite: Manufacturing and application, *Metals*, 11(12), 1919(2021). https://doi.org/10.3390/met11121919

Fayomi, J., Popoola, A. P. I., Popoola, O. M., Oladijo, O. P. and Fayomi, O. S. I., Understanding the microstructural evolution, mechanical properties, and tribological behavior of AA8011-reinforced nano-Si3N4 for automobile application, *Int. J. Adv. Manuf. Technol.*, 111(1–2), 53–62(2020). https://doi.org/10.1007/s00170-020-06054-7

Geng, R., Qiu, F. and Jiang, Q. C., Reinforcement in Al Matrix Composites: A Review of Strengthening Behavior of Nano-Sized Particles, *Adv. Eng. Mater.*, 20(9), 1–13(2018). https://doi.org/10.1002/adem.201701089

Kammer, C., Aluminum and aluminum alloys, *Springer Handb*, 157–193(2018). https://doi.org/10.1007/978-3-319-69743-7_6

Khalili, V., Heidarzadeh, A., Moslemi, S. and Fathyunes, L., Production of Al6061 matrix composites with ZrO_2 ceramic reinforcement using a low-cost stir casting technique: Microstructure, mechanical properties, and electrochemical behavior, *J. Mater. Res. Technol.*, 9(6), 15072–15086(2020). https://doi.org/10.1016/j.jmrt.2020.10.095

Kumar, M. S., Vasumathi, M., Begum, S. R., Luminita, S. M., Vlase, S. and Pruncu, C. I., Influence of B_4C and industrial waste fly ash reinforcement particles on the micro structural characteristics and mechanical behavior of aluminium (Al–Mg–Si-T6) hybrid metal matrix composite, *J. Mater. Res. Technol.*, 15, 1201–1216(2021). https://doi.org/10.1016/j.jmrt.2021.08.149

Kumar, P. and Kumar, B., Effect of T6 Heat Treatment on Mechanical and Tribological Properties of Fabricated AA7075/ZrB2/Fly Ash Hybrid Aluminum Metal Matrix Composite by Ultrasonic-Assisted Stir Casting Enroute, *Int. J. Met.*, 18(3), 2396–2414(2024). https://doi.org/10.1007/s40962-023-01177-5

Kumar, S., Dixit, G. and Dixit, S., Investigating microstructural and mechanical behavior of stir-squeeze cast TiO_2–SiC/Al6082 bimodal hybrid composites, *J. Mater. Res. Technol.*, 26, 150–163(2023). https://doi.org/10.1016/j.jmrt.2023.07.186

Manda, C. S., Babu, B. S. and Ramaniah, N., Effect of Heat Treatment on Mechanical properties of Aluminium metal matrix composite (AA6061/MoS_2), *Adv. Mater. Process Technol.*, 8(sup1), 205–222(2022). https://doi.org/10.1080/2374068X.2020.1860593

Moona, G., Walia, R. S., Rastogi, V. and Sharma, R., Aluminium metal matrix composites: A retrospective investigation, *Indian J. Pure Appl. Phys.*, 56(2), 164–175(2018).

Oyewo, A. T., Oluwole, O. O., Ajide, O. O., Omoniyi, T. E. and Hussain, M., A summary of current advancements in hybrid composites based on aluminium matrix in aerospace applications, *Hybrid Adv.*, 5, 100117(2024). https://doi.org/10.1016/j.hybadv.2023.100117

Pandiyarajan, R., Maran, P., Marimuthu, S. and Prabakaran, M. P., Investigation on mechanical properties of ZrO_2, C and AA6061 metal matrix composites, *Adv. Mater. Process Technol.*, 8(sup1), 178–186(2022). https://doi.org/10.1080/2374068X.2020.1810946

Pingale, A. D., Belgamwar, S. U. and Rathore, J. S., A novel approach for facile synthesis of Cu-Ni/GNPs composites with excellent mechanical and tribological properties, *Mater. Sci. Eng. B*, 260, 114643(2020). https://doi.org/10.1016/j.mseb.2020.114643

Ravindra., Rajesh, M., Dilip, K. K., Sailender, M., Pathalinga, P. G., Nagaraj, N. and Janaki Ramulu, P., Effect of Boron Carbide Particles Addition on the Mechanical and Wear Behavior of Aluminium Alloy Composites, *Adv. Mater. Sci. Eng.*, 2023(2023). https://doi.org/10.1155/2023/2386558

Sahu, M. K. and Sahu, R. K., Experimental Investigation, Modeling, and Optimization of Wear Parameters of B4C and Fly-Ash Reinforced Aluminum Hybrid Composite, *Front. Phys.*, 8, 1–14(2020). https://doi.org/10.3389/fphy.2020.00219

Sambathkumar, M., Gukendran, R., Mohanraj, T., Karupannasamy, D. K., Natarajan, N. and Christopher, D. S., A Systematic Review on the Mechanical, Tribological, and Corrosion Properties of Al 7075 Metal Matrix Composites Fabricated through Stir Casting Process, *Adv. Mater. Sci. Eng.*, 2023, 1-17(2023). https://doi.org/10.1155/2023/5442809

Sharma, S., Nanda, T. and Pandey, O. P., Investigation of T4 and T6 heat treatment on the wear properties of sillimanite reinforced LM30 aluminium alloy composites, *Wear*, 426–427, 27–36(2019a). https://doi.org/10.1016/j.wear.2018.12.065

Shinde, S. S. and Barve, S. B., Synthesis of A356 Matrix Hybrid Nanocomposites : Microstructural, *Mech. Tribological Character.,* 78, 230(2025). https://doi.org/10.1007/s12666-025-03697-6

Singh, N., Belokar, R. M. and Walia, R. S., A Critical Review on Advanced Reinforcements and Base Materials on Hybrid Metal Matrix Composites, *Silicon*, 14(2), 335–358(2022). https://doi.org/10.1007/s12633-020-00853-z

Tabandeh, K. M., Omrani, E., Menezes, P. L. and Rohatgi, P. K., Tribological performance of self-lubricating aluminum matrix nanocomposites: Role of graphene nanoplatelets, *Eng. Sci. Technol. Int. J.*, 19(1), 463–469(2016). https://doi.org/10.1016/j.jestch.2015.09.005